Enhanced chemiluminescent detection scheme for trace vapor sensing in pneumatically-tuned hollow core photonic bandgap fibers

Alexander M. Stolyarov,[1,2,3,10] Alexander Gumennik,[1,3,10] William McDaniel,[4] Ofer Shapira,[1,3] Brent Schell,[4] Fabien Sorin,[1,3,5] Ken Kuriki,[1,6] Gilles Benoit,[7,8] Aimee Rose,[4] John D. Joannopoulos,[1,3,9] and Yoel Fink[1,3,7,*]

[1]*Research Laboratory of Electronics, Massachusetts Institute of Technology, 77 Massachusetts Avenue, Cambridge, MA 02139, USA*

[2]*School of Engineering and Applied Sciences, Harvard University, 29 Oxford Street, Cambridge, MA 02138, USA*

[3]*Institute for Soldier Nanotechnologies, Massachusetts Institute of Technology, 77 Massachusetts Avenue, Cambridge, MA 02139, USA*

[4]*FLIR Systems, 25 Esquire Road, North Billerica, MA 01862, USA*

[5]*Current address: Laboratoire surface du verre et interfaces, Unité Mixte CNRS/Saint-Gobain UMR 125, 39 quai Lucien Lefranc, 93303 Aubervilliers, France*

[6]*Current address: CABOT Corporation, 2-5-5 Shiba Daimon, Minato-ku, Tokyo, 105-0012, Japan*

[7]*Department of Materials Science and Engineering, Massachusetts Institute of Technology, 77 Massachusetts Avenue, Cambridge, MA 02139, USA*

[8]*Current address: 3M Display & Graphics Business, 3M Center, 236-02-A-06, St. Paul, MN 55144, USA*

[9]*Department of Physics, Massachusetts Institute of Technology, 77 Massachusetts Avenue, Cambridge, MA 02139, USA*

[10]*These authors contributed equally to this work*

[*]*yoel@mit.edu*

Abstract: We demonstrate an in-fiber gas phase chemical detection architecture in which a chemiluminescent (CL) reaction is spatially and spectrally matched to the core modes of hollow photonic bandgap (PBG) fibers in order to enhance detection efficiency. A peroxide-sensitive CL material is annularly shaped and centered within the fiber's hollow core, thereby increasing the overlap between the emission intensity and the intensity distribution of the low-loss fiber modes. This configuration improves the sensitivity by 0.9 dB/cm compared to coating the material directly on the inner fiber surface, where coupling to both higher loss core modes and cladding modes is enhanced. By integrating the former configuration with a custom-built optofluidic system designed for concomitant controlled vapor delivery and emission measurement, we achieve a limit-of-detection of 100 parts per billion (ppb) for hydrogen peroxide vapor. The PBG fibers are produced by a new fabrication method whereby external gas pressure is used as a control knob to actively tune the transmission bandgaps through the entire visible range during the thermal drawing process.

OCIS codes: (060.2270) Fiber characterization; (060.2280) Fiber design and fabrication; (280.4788) Optical sensing and sensors; (170.6280) Spectroscopy, fluorescence and luminescence; (060.2370) Fiber optics sensors.

References and links

1. H. Tai, H. Tanaka, and T. Yoshino, "Fiber-optic evanescent-wave methane-gas sensor using optical absorption for the 3.392--μm line of a He-Ne laser," Opt. Lett. **12**(6), 437–439 (1987).
2. G. Stewart, W. Jin, and B. Culshaw, "Prospects for fibre-optic evanescent-field gas sensors using absorption in the near-infrared," Sens. Actuators B Chem. **38**(1-3), 42–47 (1997).
3. J. Harrington, "A review of IR transmitting, hollow waveguides," Fiber Integr. Opt **19**(3), 211–227 (2000).
4. T. Ritari, J. Tuominen, H. Ludvigsen, J. C. Petersen, T. Sörensen, T. P. Hansen, and H. R. Simonsen, "Gas sensing using air-guiding photonic bandgap fibers," Opt. Express **12**(17), 4080–4087 (2004).

#166753 - $15.00 USD Received 16 Apr 2012; revised 1 May 2012; accepted 1 May 2012; published 16 May 2012

5. A. Yildirim, M. Vural, M. Yaman, and M. Bayindir, "Bioinspired optoelectronic nose with nanostructured wavelength-scalable hollow-core infrared fibers," Adv. Mater. (Deerfield Beach Fla.) **23**(10), 1263–1267 (2011).
6. T. A. Dickinson, J. White, J. S. Kauer, and D. R. Walt, "A chemical-detecting system based on a cross-reactive optical sensor array," Nature **382**(6593), 697–700 (1996).
7. P. Yeh, A. Yariv, and E. J. Marom, "Theory of Bragg fiber," J. Opt. Soc. Am. **68**(9), 1196–1201 (1978).
8. S. G. Johnson, M. Ibanescu, M. Skorobogatiy, O. Weisberg, T. D. Engeness, M. Soljačić, S. A. Jacobs, J. D. Joannopoulos, and Y. Fink, "Low-loss asymptotically single-mode propagation in large-core OmniGuide fibers," Opt. Express **9**(13), 748–779 (2001).
9. P. Bermel, J. D. Joannopoulos, Y. Fink, P. A. Lane, and C. Tapalian, "Properties of radiating pointlike sources in cylindrical omnidirectionally reflecting waveguides," Phys. Rev. B **69**(3), 035316 (2004).
10. Y. Salinas, R. Martínez-Máñez, M. D. Marcos, F. Sancenón, A. M. Costero, M. Parra, and S. Gil, "Optical chemosensors and reagents to detect explosives," Chem. Soc. Rev. **41**(3), 1261–1296 (2012).
11. M. S. Meaney and V. L. McGuffin, "Luminescence-based methods for sensing and detection of explosives," Anal. Bioanal. Chem. **391**(7), 2557–2576 (2008).
12. S. W. Thomas 3rd, G. D. Joly, and T. M. Swager, "Chemical sensors based on amplifying fluorescent conjugated polymers," Chem. Rev. **107**(4), 1339–1386 (2007).
13. L. Zang, Y. Che, and J. S. Moore, "One-dimensional self-assembly of planar π-conjugated molecules: adaptable building blocks for organic nanodevices," Acc. Chem. Res. **41**(12), 1596–1608 (2008).
14. P. Scrimin and L. J. Prins, "Sensing through signal amplification," Chem. Soc. Rev. **40**(9), 4488–4505 (2011).
15. Y. Fink, J. N. Winn, S. Fan, C. Chen, J. Michel, J. D. Joannopoulos, and E. L. Thomas, "A dielectric omnidirectional reflector," Science **282**(5394), 1679–1682 (1998).
16. Y. Fink, D. J. Ripin, S. Fan, C. Chen, J. D. Joannepoulos, and E. L. Thomas, "Guiding optical light in air using an all-dielectric structure," J. Lightwave Technol. **17**(11), 2039–2041 (1999).
17. B. Temelkuran, S. D. Hart, G. Benoit, J. D. Joannopoulos, and Y. Fink, "Wavelength-scalable hollow optical fibres with large photonic bandgaps for CO_2 laser transmission," Nature **420**(6916), 650–653 (2002).
18. K. Kuriki, O. Shapira, S. D. Hart, G. Benoit, Y. Kuriki, J. Viens, M. Bayindir, J. D. Joannopoulos, and Y. Fink, "Hollow multilayer photonic bandgap fibers for NIR applications," Opt. Express **12**(8), 1510–1517 (2004).
19. Z. Ruff, D. Shemuly, X. Peng, O. Shapira, Z. Wang, and Y. Fink, "Polymer-composite fibers for transmitting high peak power pulses at 1.55 microns," Opt. Express **18**(15), 15697–15703 (2010).
20. D. Shemuly, A. M. Stolyarov, Z. M. Ruff, L. Wei, Y. Fink, and O. Shapira, "Preparation and transmission of low-loss azimuthally polarized pure single mode in multimode photonic band gap fibers," Opt. Express **20**(6), 6029–6035 (2012).
21. R. Deans, A. Rose, K. M. Bardon, L. F. Hancock, and T. M. Swager, "Detection of explosives and other species," Nomadics, Inc., U. S. Patent 7,799,573 B2 (2010).
22. J.-S. Yang and T. M. Swager, "Porous shape persistent fluorescent polymer films: an approach to TNT sensory materials," J. Am. Chem. Soc. **120**(21), 5321–5322 (1998).
23. J. A. Lind and G. L. Kok, "Henry's law determinations for aqueous solutions of hydrogen peroxide, methylhydroperoxide, and peroxyacetic acid," J. Geophys. Res. **91**(D7), 7889–7895 (1986).
24. F. I. Bohrer, C. N. Colesniuc, J. Park, I. K. Schuller, A. C. Kummel, and W. C. Trogler, "Selective detection of vapor phase hydrogen peroxide with phthalocyanine chemiresistors," J. Am. Chem. Soc. **130**(12), 3712–3713 (2008).

1. Introduction

Optical fibers have been applied to gas phase chemical detection due to their compact size, immunity to EM interference, and inherent adaptability for remote and distributed sensing. Absorption-based measurements relying on analyte interaction with both an evanescent field [1,2] and guided modes in hollow core fibers [3–5] have been demonstrated, as well as fluorescence-based schemes in solid-core fiber arrays [6]. In general, the detection process relies on measuring a change in fiber transmission. Typically, this change is induced by a random emergence of the analyte in the available fiber modal volume. For example, in the case of evanescent field sensing, this volume is defined by the radial extent of the evanescent wave and the length of the exposed portion of the fiber; for hollow core fibers, the available modal volume occupies the entire volume of the core. In this work, we demonstrate that by directing the analyte to preferentially overlap with the volume primarily occupied by the low-loss modes of hollow core photonic bandgap (PBG) fibers [7], rather than the entire fiber modal volume, we can direct the emission amplitude of our detection signal into those modes, and consequently enhance the sensitivity. In hollow PBG fibers the low-loss modes are found to be concentrated close the center [8]. Therefore, by positioning a chemiluminescent (CL) emitter close to the fiber center, we demonstrate a 0.9 dB/cm enhancement in sensitivity as compared to positioning the emitter on the inner fiber wall surface, where the increased

#166753 - $15.00 USD Received 16 Apr 2012; revised 1 May 2012; accepted 1 May 2012; published 16 May 2012

coupling to both higher loss core modes and cladding modes significantly reduces the fraction of light coupled to low-loss modes. Our results are consistent with numerical simulations from Bermel *et al*. [9], where the possibility of enhancing the coupling to core modes by placing a dipole emitter in the center of a cylindrical PBG structure versus on the inner surface was first predicted.

Luminescence-based detection schemes are inherently sensitive due to their demonstrated ability to produce signal gain in response to interaction with analyte; this effect is essential for detecting low (trace) levels of analytes, such as explosives [10,11]. Signal gain in organic materials can result from extended aromatic structures designed into detection materials [12], controlled self-assembly [13] and catalysis [14]. The CL scheme exploited here for peroxide detection utilizes extended aromatic structures and catalysis for gain and a transduction mechanism that offers improved chemosensing. Because the detection signal is chemically generated, no excitation source is required, which is in contrast to the traditional methods that rely on absorption and fluorescence. Compared to fluorescence, this simplification eliminates the need to filter out the excitation light from the detection signal, thus increasing sensitivity while reducing instrument complexity. Moreover, the large numerical aperture characteristic of the omnidirectional reflective surface [15,16] lining the inner fiber wall allows a larger fraction of the isotropically emitted CL to be collected and transmitted than is possible with an index guiding mechanism. Note that while hollow metallic waveguides are also characterized by omnidirectional reflectivity, their potential is hindered due to intrinsically high losses in the visible.

2. Photonic bandgap fiber fabrication and characterization

A fiber structure with sub-100 nm layer thicknesses is necessary to confine the visible wavelengths emitted by our sensing material. However, owing to the fabrication challenges in maintaining structural integrity at the nanometer scale and in reducing scattering defects, low-loss, high-index-contrast PBG fibers have only been produced to transmit in the infrared (IR) to near-IR [17–20] where feature sizes are larger and wavelengths are less sensitive to scattering sites. Here we report on low-loss (<5 dB/m), hollow core omnidirectional PBG fibers with fundamental bandgaps spanning the visible spectrum. Note that while it is possible to use higher order bandgaps of IR fibers to transmit visible light, these bandgaps do not exhibit omnidirectional reflectivity for the materials considered here, and consequently are characterized by a lower numerical aperture.

The fibers are thermally drawn from preforms containing 15 bilayers of As_2S_3 and polyetherimide (PEI) and clad by PEI. The general process of preparing these multimaterial PBG fiber preforms has been reported on previously [17–20]. Here, to reduce the fiber transmission losses, which scale inversely with the core radius [8], we implement a new fabrication approach for producing fibers with large cores for visible light transmission. Rather than introducing pressure into the preform merely to keep it from collapsing (as was done previously), here we use the pressure as a control knob to tune the bilayer thickness during the draw with nanometer scale resolution. At a constant draw speed, increasing the pressure compresses the multilayer structure, consequently blue-shifting the transmission bandgap while increasing the core diameter (Figs. 1(a) and 1(b)).

#166753 - $15.00 USD Received 16 Apr 2012; revised 1 May 2012; accepted 1 May 2012; published 16 May 2012

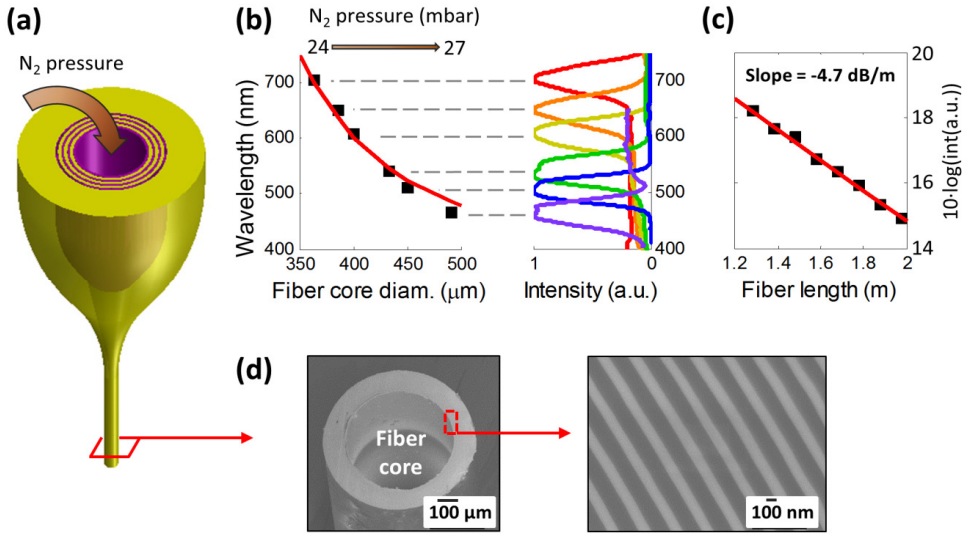

Fig. 1. (a) Schematic of the new pneumatically tunable photonic bandgap (PBG) fiber drawing process. The brown arrow denotes the introduction of nitrogen gas pressure into the preform core during the thermally-induced scaling of the preform. The purple layers correspond to As_2S_3 glass and the yellow corresponds to polyetherimide (PEI). (b) The bandgap peak positions are plotted as a function of the fiber core diameter. In contrast to the normal drawing process in which the bandgap redshifts with increasing diameter, here the bandgap blueshifts with increasing diameter. The red curve is the center bandgap position calculated by the transfer matrix method. The full transmission bandgap spectra are shown on the right. The brown arrow denotes the increase in nitrogen pressure that is supplied to the preform core during the draw in order to achieve the desired effect of increasing the core diameter while blue-shifting the transmission bandgap. (c) A typical cutback measurement depicted for a fiber with a bandgap centered at 532 nm, demonstrating losses of 4.7 dB/m. (d) Scanning Electron Microscope (SEM) micrographs of a large core PBG fiber (left) fabricated with the described method and a zoomed view of the multilayer PBG structure lining the core (right).

A cutback measurement performed on a 2 m long fiber sample with a core diameter of 430 μm and transmission peak centered near 532 nm reveals a loss of 4.7 dB/m (Fig. 1(c)) for the 532 nm line of an Nd:YAG laser. The structure of the fibers was evaluated with a high resolution scanning electron microscope (SEM, JEOL 6700F) (Fig. 1(d)). Remarkably, despite the fact that pressure was used to compress the layers during the draw, they maintain their form at the nanometer scale along meters of fiber. Note that while a seemingly trivial alternative approach to producing large-core fibers is to start with a large inner diameter on the preform level, the practical limitations on the pre-drawn bilayer film length and thickness make this approach difficult to implement without compromising the number of bilayers in the multilayer structure.

3. Optofluidic chemiluminescent detection setup

The hollow core PBG fiber simultaneously performs multiple functions in our chemical detection scheme. It hosts the CL sensing material inside the core, and concurrently intakes and transports the analyte being detected. Furthermore, the fiber transmits light generated from the analyte-sensing event at the front end to the distal end for detection (Fig. 2(a)) and can optically isolate that detection signal from ambient light and other sources of background noise. In order to maximize the fiber's transmission efficiency, the peak of the PBG transmission is designed to match the CL emission spectrum (Fig. 2(b)). Note that while here we choose to work with an oxamide-based peroxide detection material which emits in the

#166753 - $15.00 USD Received 16 Apr 2012; revised 1 May 2012; accepted 1 May 2012; published 16 May 2012

green [21], the spectral tunability of the PBG structure allows the described methods to be applied for sensing of other chemical species, such as e.g., fluorescence-based TNT detection [22].

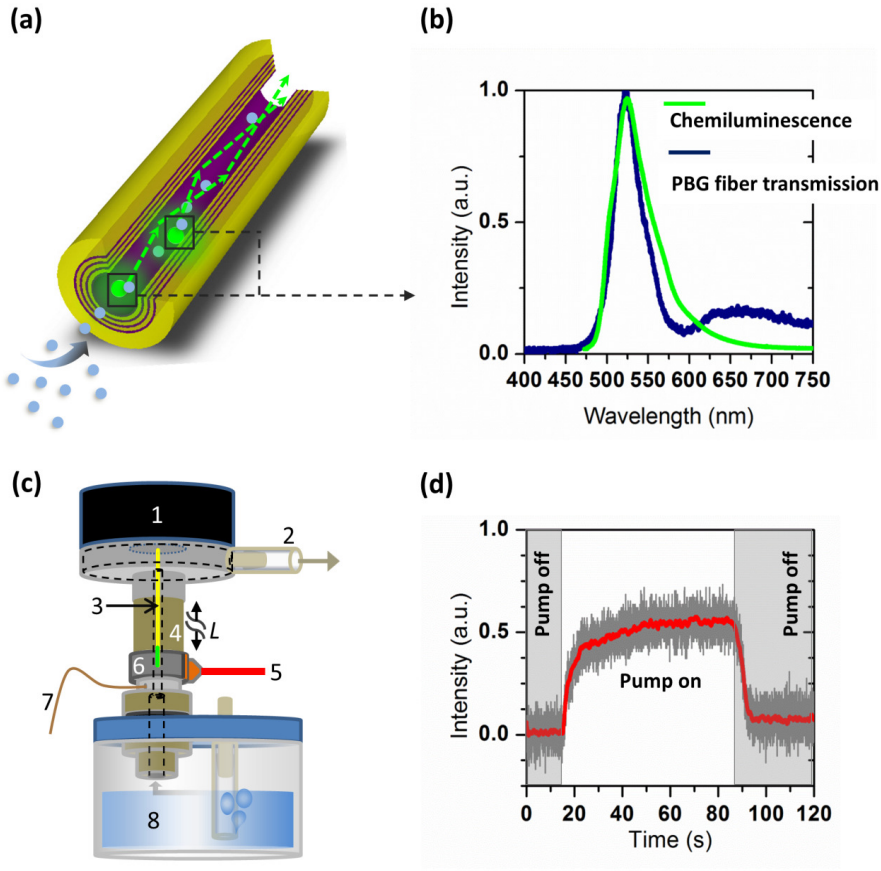

Fig. 2. (a) Schematic drawing demonstrating the principle of using a hollow core PBG fiber for CL detection of peroxide vapors. When peroxide (light blue spheres) interacts with the sensing material (green spheres), luminescence is generated and guided by the PBG structure along the fiber length to the distal end for detection. (b) The peak of the fiber transmission bandgap is selected to coincide with the peak of the CL in order to most efficiently capture and transmit the emitted light. (c) Schematic of the custom built optofluidic system used for controlled delivery of peroxide vapor into the fiber core and simultaneous measurement of the transmitted detection signal. The system components include: (1) optical detector, (2) outlet for connecting to a syringe pump, (3) hollow core PBG fiber (yellow) with peroxide sensing material (green) immobilized in the core, (4) extension pieces of variable lengths to accommodate different fiber lengths, (5) heating element (Minco) used to catalyze the CL reaction, (6) clamp used to compress the heating element against the casing which contains the fiber tip, (7) thermocouple used for monitoring the temperature, and (8) container with an aqueous peroxide solution of known concentration. (d) A plot depicting a typical measurement. When the syringe pump is turned on, peroxide vapor flows through the fiber core resulting in the rise of the CL signal, which reaches a plateau. The signal returns back to the baseline when the syringe pump is turned off. The displayed measurement is for a peroxide concentration of 1% (aqueous).

We designed and constructed a custom optofluidic system to measure CL intensity while controlling flow of peroxide vapor through the fiber core (Fig. 2(c)). The setup consists of a hydrogen peroxide solution of known concentration prepared from a 35% standard (Sigma-Aldrich). Air is bubbled though this solution at a controlled rate by generating suction with an automated syringe pump, thus ensuring that the headspace is saturated with peroxide vapor at

#166753 - $15.00 USD Received 16 Apr 2012; revised 1 May 2012; accepted 1 May 2012; published 16 May 2012

all times during a measurement. The fiber tip, which contains the sensing material, is heated to ~90°C to catalyze the CL reaction. Extensions of variable lengths are used to accommodate fibers of different lengths so that cutback measurements can be performed. The distal end of the fiber is sealed against a holder which contains a port for connecting the syringe pump and a transparent glass window for transmitting the light to an optical detector (Newport 818 series detector with 2935-C power meter). The fiber is hermetically sealed with an o-ring to ensure that the peroxide rich vapor can only pass through the core (or through the hollow capillary immobilized in the core as will be discussed later).

A typical measurement that is performed using the described setup is shown in Fig. 2(d). No optical signal is measured when the syringe pump is in the off state. Upon activating the pump to a speed of 50 ml/min, a fast rise (~seconds) in intensity is observed which lasts as long as the pump is on. When the syringe pump is turned off, the signal rapidly drops (~seconds) back to the baseline.

4. Results

To probe the effect of spatially varying the location of the CL reaction within the hollow core fiber on the efficiency of coupling the resulting emission to low-order fiber transmission modes, two geometric configurations are explored. For both configurations, a PBG fiber with a transmission bandgap centered near 530 nm with a core diameter of 530 μm was fabricated using the method described in section 2. In the first (conFig. 1), the CL sensing material is coated directly on the inner fiber surface for a length of 1.5 cm (Fig. 3(a, top)). This coating process is achieved by dipping the fiber tip into the sensing material (which is initially in a liquid state and heated to 60°C on a hotplate) and removing the liquid plug by applying a steady flow of air using a syringe pump. The fiber is then dried under vacuum at room temperature to remove any remaining solvent, leaving only a thin (~7 μm) CL film coating on the fiber, as determined by optical microscopy of the fiber cross section.

In the second configuration (conFig. 2), the sensing material is removed from the wall (Fig. 3(b, top)) by coating it on the inside of a hollow glass capillary clad by polyimide (PI) (ID = 320 μm, OD = 450 μm, Polymicro Technologies) using the same procedure as described above. The capillary is immobilized in the center of the fiber by a custom-made stainless steel bushing which holds the capillary by friction. The opaque PI coating on the portion of the capillary which is inserted into the PBG fiber is removed with a flame prior to coating the sensing material so that the CL emission is not absorbed by it. The total length of capillary which fits inside the PBG fiber is 1.5 cm. The outside of the PBG fiber is sealed with an o-ring which is compressed by the bushing to ensure that peroxide vapor only flows through the hollow capillary.

We hypothesize that conFig. 2 is the favorable architecture for improving the coupling of the CL to low-loss modes for two reasons. First, since the sensing material is close to the center of the fiber, the overlap in intensity between the CL emission and the intensity distribution of the PBG fiber fundamental modes is enhanced. Second, part of the emitted light is expected to couple to the highly lossy cladding modes when the high-index CL film ($n \approx 1.7$) is coated directly on the inner fiber surface (conFig. 1).

To test our hypothesis, four fiber samples were measured in the optofluidic system for each of the two configurations described above, with a peroxide flow rate of 50 ml/min and a concentration of 1% (aqueous). The CL intensity was measured for different fiber lengths in 1 cm increments starting with a length of 8.8 cm and ending with 3.8 cm. For each cut after the first 8.8 cm measurement, the optical detector portion of the setup is temporarily disconnected, a 1cm extension piece is removed, the fiber is carefully cleaved using a custom-made polymer fiber cleaver, and the detector is reconnected. Figures 3(a, bottom) and 3(b, bottom) depict the averaged results for conFigs. 1 and 2, respectively. Note that the data is corrected for the differences in surface areas between the two coatings to facilitate the

#166753 - $15.00 USD Received 16 Apr 2012; revised 1 May 2012; accepted 1 May 2012; published 16 May 2012

comparison. These cutback measurement results are analyzed using a multimode fiber transmission model described in the following section.

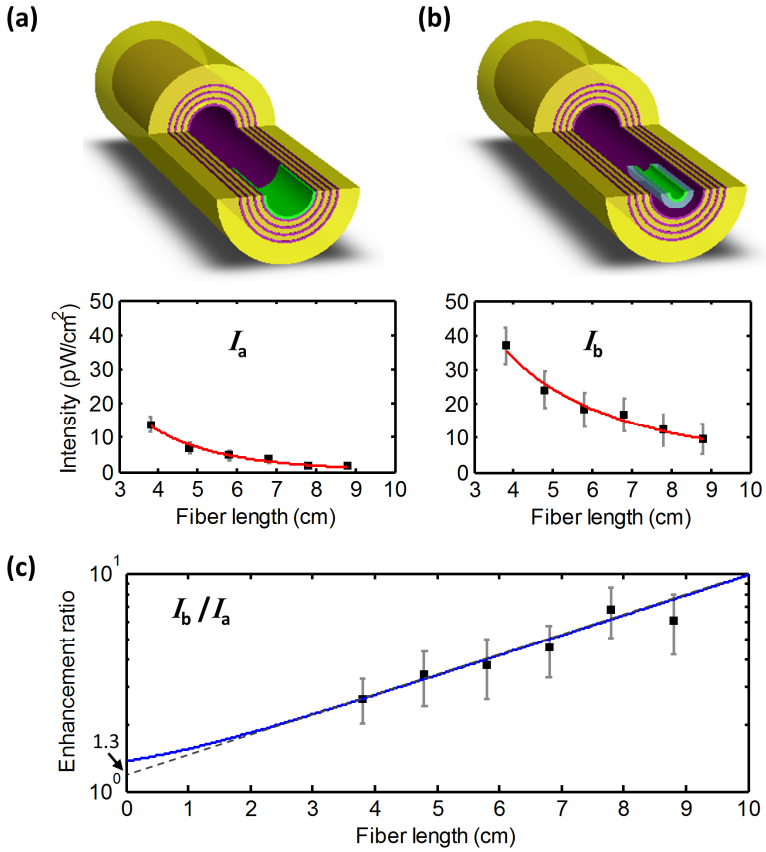

Fig. 3. (a, top) Schematic of the detection configuration in which the CL material is coated directly on the inner fiber surface (conFig. 1). (a, bottom) Results of cutback measurements are the black points and the fit to the data is in red. (b, top) Schematic of the detection configuration in which the CL material is coated onto a hollow glass capillary which is fixed in the center of the fiber (conFig. 2). The bushing which holds the capillary is omitted in the drawing for clarity. In our setup, the peroxide vapor only flows through the capillary core and not around it. (b, bottom) Results of cutback measurements are the black points and the fit to the data is in red. Cutback measurements are performed for multiple samples in each configuration using the setup described in Fig. 2(c), with a peroxide concentration of 1% (aqueous). (c) The black points correspond to the ratio of the data presented in (a, bottom) and (b,bottom) and the blue curve is the ratio of the fits shown in red (I_b/I_a). The extrapolated ratio of 1.3 at 0 cm arises from the fact that part of the light coated on the PBG surface escapes to the cladding.

5. Multimode fiber transmission model

Our aim is to quantify the improvement in fiber performance by implementing conFig. 2 versus conFig. 1 as a detection scheme. The intensity at position z of a multimoded waveguide can be expressed as a sum over each of the modes:

$$I(z) = \sum_m A_m e^{-\alpha_m z} = \int_m A_m e^{-\alpha_m z} dm \qquad (1)$$

where A_m is the intensity coupled into a particular fiber mode m with a propagation loss α_m. To proceed in evaluating the integral in Eq. (1), the following two assumptions are made. First,

#166753 - $15.00 USD Received 16 Apr 2012; revised 1 May 2012; accepted 1 May 2012; published 16 May 2012

since the CL emits in all directions and with a random phase and polarization, the function describing the coupling efficiency into the spectrum of modes is expected to be smooth. As a zero order approximation, we assume that the coupling of the CL emission into the fiber modes is uniformly distributed, with an upper and lower mode cutoff. Second, we assume that the propagation losses of these modes scale linearly with the mode number. We verify that this relationship holds true by calculating the losses of the first 70 hybrid modes using the Leaky mode technique [8].

Using the above two assumptions, Eq. (1) can be simplified to:

$$I(z) = \int_{m_1}^{m_2} \frac{I_0}{m_2 - m_1} e^{-\alpha_0 m z} dm \tag{2}$$

where I_0 is the total intensity which is equally distributed among all of the participating modes, α_o is the loss of the lowest order fundamental HE_{11} mode (estimated to be ~$2x10^{-4}$ cm^{-1} by applying core-size scaling laws [8] to losses of individual modes measured on similar fibers with smaller cores), and m_2 and m_1 are the upper and lower mode cutoffs, respectively. The integral in Eq. (2) can be analytically computed, resulting in:

$$I(z) = \frac{I_0}{(m_2 - m_1)} \cdot \frac{1}{\alpha_0 z} (e^{-m_1 \alpha_0 z} - e^{-m_2 \alpha_0 z}) \tag{3}$$

The red curves in Figs. 3(a, bottom) and 3(b, bottom), denoted $\boldsymbol{I_a}$ and $\boldsymbol{I_b}$, respectively, are fits of Eq. (3) to the data. We note that a mutual dependence exists between I_0 and m_2, therefore one of them must be fixed. Our strategy is to continue to increase m_2 until further increase does not yield any improvement in the fit. This value of m_2 thus corresponds to the minimum number of modes that are needed to describe the measured intensity after 3.8 cm of propagation (the shortest length that was measured). The lower mode cutoff, m_1, on the other hand, reveals the efficiently of coupling to the lower order modes, which are still present after 8.8 cm of propagation. We note that this value is not affected by changes in I_0 and m_2. For conFigs. 1 and 2, m_1 was found to be 1600 $\pm$ 200 and 500 $\pm$ 100 modes, respectively, and m_2 was determined to be 8200 ± 500 modes for both. Thus, as hypothesized, the coupling to lower order modes can be improved by removing the CL material off of the wall.

The enhancement ratio $\boldsymbol{I_b/I_a}$, plotted in Fig. 3(c), quantifies the relative improvement in the transmitted intensity, which is determined to be 0.9 dB/cm in the range of 3.8 – 8.8 cm. We can access the situation at the front of the fiber (at z = 0 cm) by letting m_2 grow very large to account for the fact that the number of excited modes can be on the order of a million in this fiber (core diameter ~1000λ). This is performed graphically in Fig. 3(c), where the ratio is extrapolated to z = 0 from the linear portion of the plot, which describes the situation after 3.8 cm of propagation. An enhancement ratio of 1.3 (and not 1) reveals that a portion of the light in conFig. 1 escaped to the cladding, as predicted.

Note that only hybrid modes were considered in the described model. The results are expected to change only minimally if pure TE and TM modes are included since they represent only a small fraction of all the available modes. These modes were omitted because the difference in losses between pure TE and TM modes with identical quantum numbers is much larger than the difference for the hybrid HE and EH modes.

6. Sensitivity measurement

To demonstrate trace level vapor detection, we quantify the sensitivity of our fiber-based stand-off chemical sensor with a 5.8 cm long fiber (Fig. 4), containing a coated insert (1.5 cm long) as described above (conFig. 2). Known concentrations of peroxide were diluted with DI water from a 35% (aqueous) standard, and the vapor phase concentration in the headspace from each solution was determined using Henry's law [23]. A limit of detection of 100 ppb (at SNR = 1) was achieved with the described setup.

#166753 - $15.00 USD Received 16 Apr 2012; revised 1 May 2012; accepted 1 May 2012; published 16 May 2012

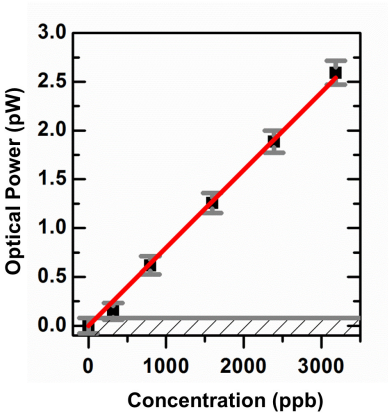

Fig. 4. Sensitivity measurement for peroxide vapor performed using a 5.8 cm long fiber with the sensing material coated as in conFig. 2 (see Fig. 3(b, top)). The horizontal grey line at the bottom is the noise of the optical detector. The limit of detection is 100 ppb at SNR = 1.

7. Conclusions

We demonstrate that by sculpting a CL emission volume within a hollow core photonic bandgap fiber, we can preferentially restrict its coupling to lower order fiber modes, thereby increasing detection sensitivity to peroxide vapors by 0.9 dB/cm. Further improvement to sensitivity can be achieved by optimizing the position of the CL material inside the fiber core, for example, by positioning it even closer to the center. To increase specificity of mode selection using this method, waveguide dimensions can be scaled down in order to increase the separation between adjacent modes. For instance, a waveguide which supports only four modes would enable selective coupling of the CL intensity to either the Gaussian-like fundamental modes (HE_{11} and EH_{11}) or doughnut-like modes (TE_{01} and TM_{01}) with a high specificity. These approaches can enable more sensitive fiber detectors, multi-analyte sensing in a single fiber, spatial mapping of sensing events inside hollow waveguide structures for more selective detection, as well as Purcell enhanced fluorescence detection schemes [9]. The study presented herein marks an important step in the development of fiber-optic peroxide sensors for stand-off monitoring of environmental, health, and most notably, security hazards, given the rising illegal use of peroxide-based explosives [24].

Acknowledgments

The authors thank Prof. Steven Johnson for fruitful discussions. Alexander M. Stolyarov acknowledges support from the US National Science Foundation Graduate Research Fellowship. Alexander Gumennik acknowledges the Yad Hanadiv fund for financial support (Rothschild fellowship). This work was supported in part by the Materials Research Science and Engineering Program of the US National Science Foundation under award number DMR-0819762 and also in part by the US Army Research Office through the Institute for Soldier Nanotechnologies under contract number W911NF-07-D-0004.

#166753 - $15.00 USD Received 16 Apr 2012; revised 1 May 2012; accepted 1 May 2012; published 16 May 2012